The Electrochemical Properties and Mechanism of Formation of Anodic Oxide Films on Mg-Al Alloys

Seong-Jong Kim* and Masazumi Okido*

Graduate School of Engineering, Nagoya University, Furo-cho, Chikusa-ku, Nagoya 464-8603, Japan
Received March 24, 2003

The electrochemical properties and the mechanism of formation of anodic oxide films on Mg alloys containing 0-15 mass% Al, when anodized in NaOH solution, were investigated by focusing on the effects of anodizing potential, Al content, and anodizing time. The intensity ratio of $Mg(OH)_2$ in the XRD analysis decreased with increasing applied potential, while that of MgO increased. $Mg(OH)_2$ was barely detected at 80 V, while MgO was readily detected. The anti-corrosion properties of anodized specimens at each constant potential were better than those of non-anodized specimens. The specimen anodized at an applied potential of 3 V had the best anti-corrosion property. The intensity ratio of the β phase increased with aluminum content in Mg-Al alloys. During anodizing, the active dissolution reaction occurred preferentially in β phase until about 4 min, and then the current density increased gradually until 7 min. The dissolution reaction progressed in α phase, which had a lower Al content. In the anodic polarization test in 0.017 mol·dm^{-3} NaCl and 0.1 mol·dm^{-3} Na_2SO_4 at 298 K, the current density of Mg-15 mass% Al alloy anodized for 10 min increased, since the anodic film that forms on the α phase is a non-compacted film. The anodic film on the α phase at 30 min was a compact film as compared with that at 10 min.

Key Words : Anodizing, Electrochemical properties, Mg-Al alloys, Anti-corrosion property

Introduction

Of the common metals, magnesium has the lowest density; it also has excellent specific strength. Magnesium must be surface treated to prevent corrosion, since it is a very active metal electrochemically. There are many ways to treat the surface of magnesium and its alloys, including anodizing, painting, and electroplating. Dow 17 bath is generally used to anodize magnesium alloys in the commercial chemical industry. However, Dow 17 bath, which contains chromate and fluoride, causes many problems for humans and the environment, and is difficult to recycle. Furthermore, it is deemed a Class 1 carcinogenic substance in the Pollutant Release and Transfer Register (PRTR).[1] In Europe, the use of lead, mercury, cadmium, and Cr^{+6} in electronic products is prohibited. A waste electrical and electronic equipment (WEEE) collection plan was announced in June 2000. The use of Cr^{+6} will gradually be phased out, and prohibited by the year 2007.[2] In addition, the environmental load value (ELV) order restricting the use of environmental load substances will be implemented incrementally, beginning in July 2003. The use of Cr^{+6} by the automobile industry is prohibited after July 2007.[3] We have therefore been investigating alternatives to chromate baths for Mg alloys.[4-7] Anodizing magnesium alloys generates multi-porous films several tens of micrometers thick. The anodic behavior of magnesium in NaOH solutions at a wide range of potentials was first described in the studies of Emley,[8] Huber,[9] and Evangelides.[10] Only a few investigations have examined the growth behavior of anodic oxide surface films on magnesium,[8] Mg-Al alloys,[9,11-13] and aluminum.[14] Khaselev *et al*. reported the anodic behavior of binary Mg-Al alloys in KOH solutions over a wide range of applied potentials, emphasizing the effect of aluminum content on the passivation phenomena and spark potential.[13] It has also been reported that the effect on an anodizing film of aluminum ions in the solution is more remarkable than that of the Al added to Mg-Al alloys. The current density during anodizing effectively decreases with increasing AlO_2^- content in the solution.[15,16]

This study characterized anodic oxide films, using parameters such as the anodizing potential, anodizing time, and Al content of Mg-Al alloys in 1.0 mol·dm^{-3} NaOH solution at 298 K, and the mechanism of anodic oxide film formation. The anodized film was analyzed using electrochemical techniques: scanning electron microscopy (SEM), X-ray diffraction analysis (XRD), and energy dispersive X-ray spectrometry (EDX).

Experimental Section

Mg-Al alloys were prepared by melting a mixture of pure metals at 1073 K and allowing the mixture to solidify rapidly. This process was repeated twice to prevent segregation of the aluminum. The homogeneous distribution of Al in the alloy was confirmed by ICP-AES (SPS-1500 VR). The purity of the prepared alloy was 99.9 mass% for Mg and 99.999 mass% for Al. Alloy electrodes were mounted using epoxy resin, leaving an exposed area of 100 mm^2, and polished with 0.05-μm alumina powder. The specimens were carefully degreased with acetone and water. The constant potential experiment system consisted of a Pt coil as a counter electrode, and an Ag/AgCl sat. KCl reference

*Corresponding author. E-mail: kim@f2.numse.nagoya-u.ac.jp

electrode. The experiments were conducted in 250 mL of 1 mol·dm^{-3} NaOH alkaline solution at 298 K. The distance between the working and counter electrodes was approximately 50 mm. The solution was stirred during all of the experiments. The Mg alloys were anodized at constant potentials of 3, 10, 40, and 80 V. The anodic polarization curves of specimens anodized at various potentials were measured in a solution containing 0.017 mol·dm^{-3} NaCl and 0.1 mol·dm^{-3} Na_2SO_4 at 298 K at a scan rate of 1 mVs^{-1}, in order to characterize the corrosion resistance of the anodizing films. The anodizing films were also evaluated using SEM, XRD, and EDX.

Results and Discussion

First, the Al content at the surface of the Mg-Al alloys was examined using XRD. Figure 1(a) shows typical XRD patterns of Mg-Al alloys containing 1.5, 3, 7, and 9 mass% Al before anodizing. Magnesium and $Mg_{17}Al_{12}$ were clearly detected in the XRD results. $Mg_{17}Al_{12}$ is intermetallic compound of 99.9 mass% for Mg and 99.999 mass% for Al. This intermetallic compound, $Mg_{17}Al_{12}$, is β phase. Mg which not formed intermetallic compound is α phase. The highest peaks of Mg and $Mg_{17}Al_{12}$ correspond to 36.8, and 43.6°, respectively. The intensity ratio, R, of $Mg_{17}Al_{12}$/Mg is defined as the ratio at 43.6 to 36.8°. Figure 1(b) shows the change in R in the alloys. The intensity ratio of $Mg_{17}Al_{12}$ increased with increasing Al content in the Mg-Al alloys. $Mg_{17}Al_{12}$ peaks were barely detected in the Mg-Al alloys containing less than 3 mass% Al. It was not detected intermetallic compound in 1.5 mass% Al, and 3 mass% Al. However, intermetallic compound in 7 mass% Al was detected from XRD pattern. Therefore, Mg-Al alloys containing over 7 mass% Al were composed of α phase, *i.e.*, Mg, and β phase, *i.e.*, $Mg_{17}Al_{12}$.

Before anodizing treatment at a constant potential in 250 mL NaOH solution, anodic polarization was conducted at a scan rate of 60 mVs^{-1} at 298 K to investigate the potentials of the active dissolution reaction, passivation, and sparking on the alloys. An anodic current increment corresponding to

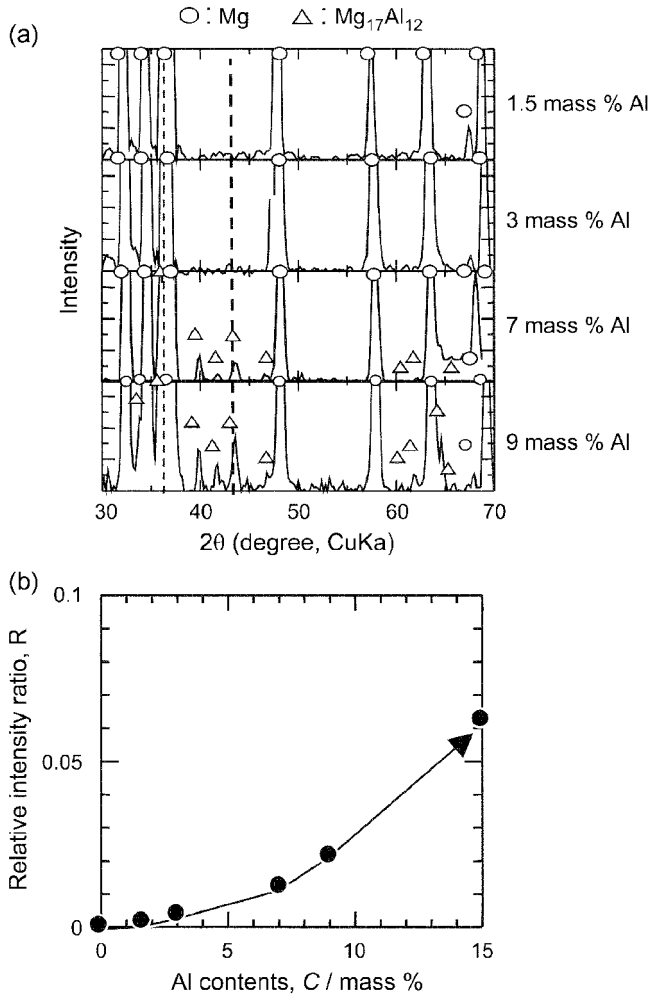

Figure 1. Surface analysis by XRD of Mg-Al alloys with Al contents.

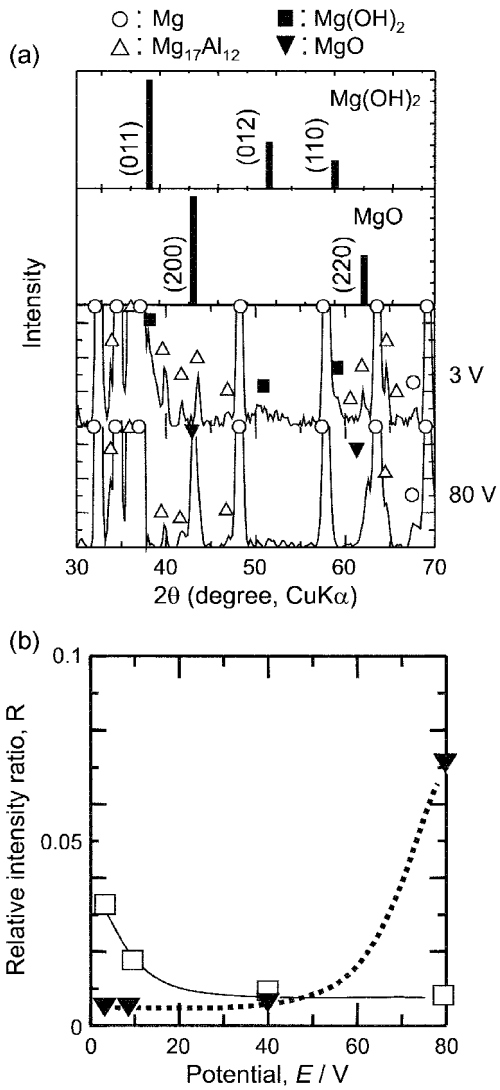

Figure 2. XRD analysis of specimens of Mg-9 mass% Al alloy anodized for 10 min at various constant potentials in 1.0 mol·dm^{-3} NaOH solution at 298 K.

the active dissolution reaction and the formation of hydroxide, $Mg = Mg^{2+} + 2e^-$, $Mg^{2+} + 2OH = Mg(OH)_2$, was observed at potentials between 3 and 7 V for all specimens.[5] Breakdown with intense sparking was observed at above 80 V.[8]

Next, constant potential anodizing was carried out in 1.0 mol·dm^{-3} NaOH solution at 298 K. Figure 2(a) shows the XRD patterns of Mg-9 mass% Al anodized for 10 min at various potentials. Peaks of $Mg(OH)_2$ and MgO were also detected in the XRD analysis. $Mg(OH)_2$ predominated at an applied potential of 3 V, while MgO appeared at an applied potential of 80 V. The highest peaks of Mg, $Mg(OH)_2$, and MgO correspond to 36.8, 38.0, and 43.0°, respectively. The intensity ratio was calculated in the same manner as in Figure 1. Figure 2(b) shows the intensity ratio at each applied potential. The intensity ratio of $Mg(OH)_2$ decreased with increasing applied potential, while that of MgO increased. $Mg(OH)_2$ was barely detected at 80 V, while MgO was strongly detected. These trends were similar to the case of Mg-3 mass% Al.

Figure 3 shows surface photographs of Mg-9 mass% Al anodized at various potentials for 10 min. The surface was rough at 3 V, due to $Mg(OH)_2$ generated by the surface dissolution reaction. The surface dissolution reaction occurred selectively on the α phase only (white area). The α phase tarnished, due to a dissolution reaction that was minimal on β phase. Surfaces anodized at 3, 10, and 80 V had roughnesses of approximately 1.2, 0.60, and 0.12 μm, respectively.[17] The surfaces of specimens anodized at 40 and 80 V were comparatively flat. In addition, the surface of Mg-3 mass% Al anodized at 3 V was very rough, similar to Mg-9 mass% Al, and was dark gray in color. When anodized at 10 V, the difference in the dissolution reaction of the α and β phases was very distinct.

Next, the corrosion behavior of the surface films was examined. Figure 4 shows the anti-corrosion properties in a solution containing 0.017 mol·dm^{-3} NaCl and 0.1 mol·dm^{-3} Na_2SO_4 at 298 K. The specimens used were Mg-9 mass% Al alloy anodized for 10 min at various potentials at 298 K in 1 mol·dm^{-3} NaOH solution. The anti-corrosion properties of the anodized specimens at each constant potential were better than those of non-anodized specimens. The specimen anodized at an applied potential of 3 V had the best anti-corrosion properties because there was a large shift in potential in the noble direction with increasing corrosion current. Corrosion potential defined the potential at which the current density reached 0.1 mA·cm^{-2} in 9 mass% Al from anodic polarization curve of Figure 4, and compared corrosion potentials between the various alloys as an indicator of corrosion resistance. Corrosion potentials in pure Mg, Mg-3 mass % Al calculated in same manner with 9 mass % Al.

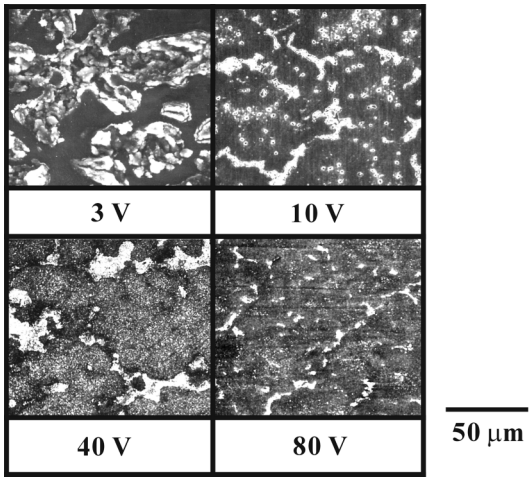

Figure 3. SEM photographs of Mg-9 mass% Al alloy specimens anodized for 10 min at various constant potentials in 1.0 mol·dm^{-3} NaOH solution at 298 K.

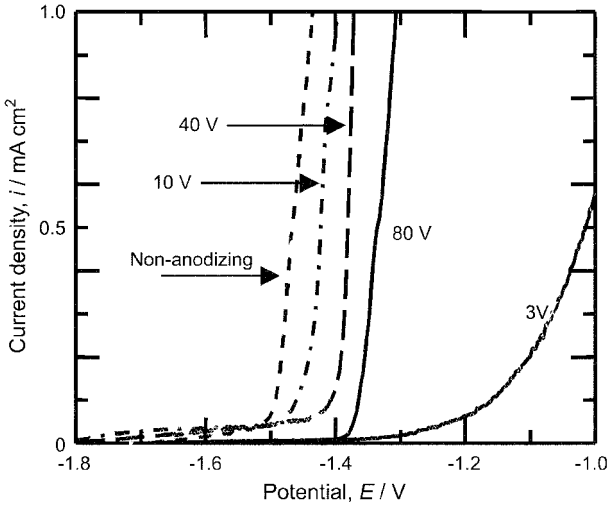

Figure 4. Comparison of the anti-corrosion properties in 0.017 mol/dm^3 NaCl and 0.1 mol·dm^{-3} Na_2SO_4 solution at 298 K. The used specimen is Mg-9 mass% Al alloy anodized for 10 min at various constant potentials.

Table 1 summarizes the potential, E_{corr}, corresponding to a current density of 0.1 mA·cm^{-2} for pure Mg, Mg-3 mass% Al, and Mg-9 mass% Al alloys. The anodized films degraded at current densities above 0.2 mA·cm^{-2}. To evaluate the anodic films before they degraded, we compared the potentials at a current density of 0.1 mA·cm^{-2}. The anti-corrosion property of Mg-9 mass% Al was better than that of Mg-3 mass% Al alloy. Al has a beneficial effect on the passivity, which leads to the high corrosion resistance of Mg-Al alloys.[1819] The best anti-corrosion effect was obtained with anodizing at 3 V, and the next best at 80 V. Therefore, anodizing potentials of 3 and 80 V were used in the subsequent experiments.

The current densities of alloy specimens anodized for 10

Table 1. Comparison of E_{corr} corresponding to a current density of 0.1 mA·cm^{-2}

Anodized potential	Non-anodizing	3 V	10 V	40 V	80 V
Pure Mg	-1.670 V	-1.726 V	-1.741 V	-1.747 V	-1.720 V
Mg-3 mass% Al	-1.518 V	-1.250 V	-1.500 V	-1.467 V	-1.395 V
Mg-9 mass% Al	-1.490 V	-1.160 V	-1.455 V	-1.410 V	-1.369 V

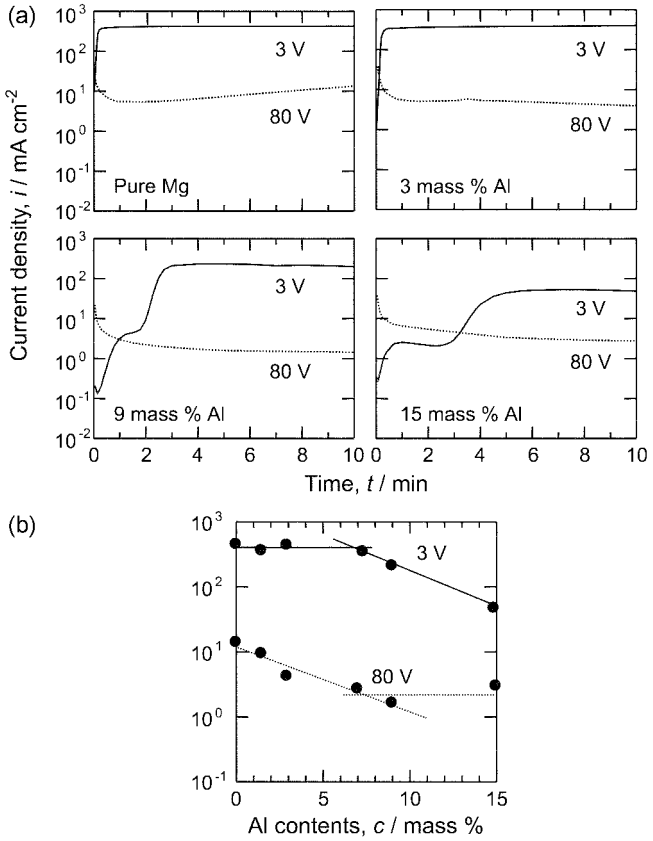

Figure 5. Comparison of the current density after anodizing for 10 min with Al contents in 1.0 mol·dm^{-3} NaOH solution at 298 K.

min in 1.0 mol·dm^{-3} NaOH solution at 298 K are compared in Figure 5. As shown in Figure 5(a), stagnation of the current density for 9 mass% Al in the case of 3 V occurred at a current density of about 2 mA·cm^{-2}. The stagnation time increased with the aluminum content, resulting in a decrease in the current density after 10 min (Figure 5(b)). The plateau phenomenon in 15 mass% Al will treat in Figure 8. Moreover, at 80 V, the current density after 10 min decreased with 9 mass% Al, but was slightly higher with 15 mass% Al.

Figure 6 shows anodic polarization curves in 0.017 mol·dm^{-3} NaCl and 0.1 mol·dm^{-3} Na_2SO_4 at 298 K. Specimens with different Al contents were anodized at an applied potential of 3 V in 1 mol·dm^{-3} NaOH for 10 min at 298 K. The potential shifted in the noble direction with increasing aluminum content, while the polarization curve of Mg-15 mass% Al had a distinct shape. The potential of 15 mass% Al for current densities of 0.15-2.3 mA·cm^{-2} was lower than that of 9 mass% Al. The photographs of the anodized surface show that dissolution of the α phase occurred at an applied potential of 3 V regardless of the Al content. The α phase in 15 mass% Al took the form of a large hole. Moreover, the two-step current plateau increase was insufficient with anodizing for 10 min. Consequently, Mg-15 mass% Al was anodized for 30 min at 3 V in 1 mol·dm^{-3} NaOH at 298 K.

Figure 7 shows the changes in current (a) and surface morphology (b) with time on anodizing at 3 V of 15 mass% Al in 1 mol·dm^{-3} NaOH at 298 K. The current density was

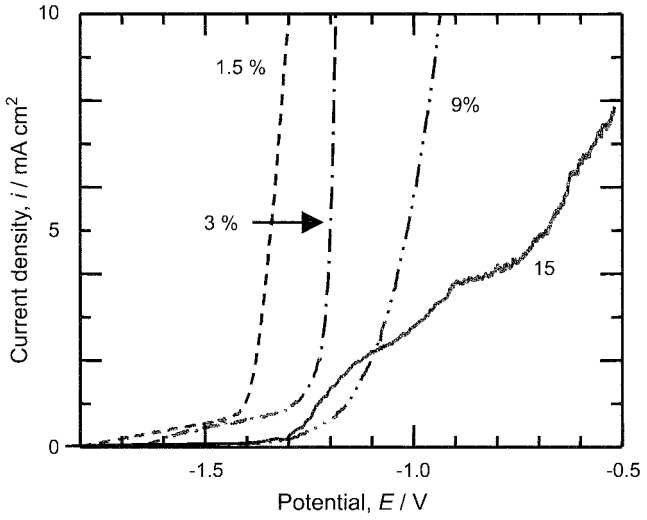

Figure 6. Anodic polarization curves in 0.017 mol·dm^{-3} NaCl and 0.1 mol·dm^{-3} Na_2SO_4 solution at 298 K. The specimens were anodized at an applied potential of 3 V with Al contents 1 mol·dm^{-3} NaOH solution for 10 min at 298 K.

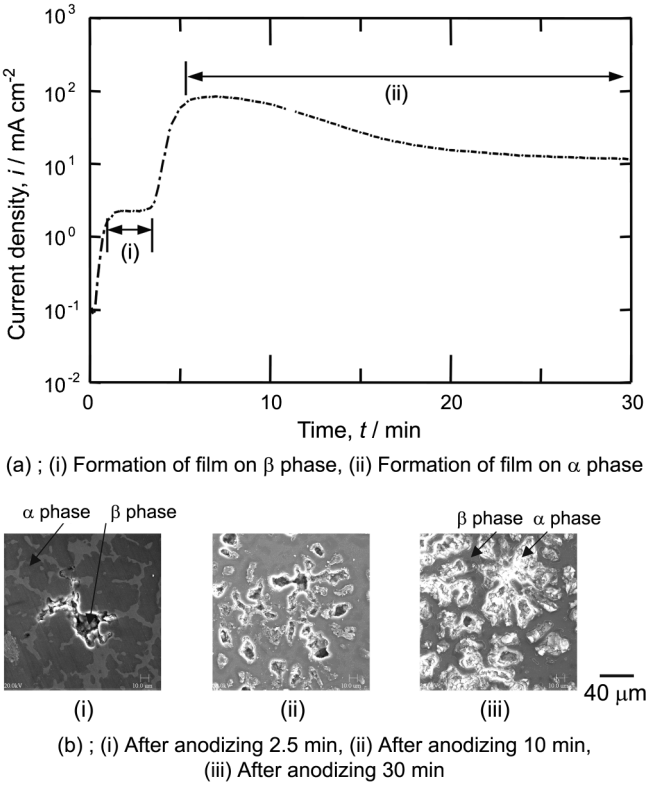

Figure 7. Effect of anodizing time affecting to i-t curves and surface morphologies in anodizing at an applied potential of 3 V for 15 mass% Al in 1.0 mol·dm^{-3} NaOH solution at 298 K.

maximal at an anodizing time of 7 min. Thereafter, the current density gradually diminished and was about 10 mA·cm^{-2} after 30 min. It seemed that an anodizing film formed via a dissolution reaction on the β phase at 2 mA·cm^{-2} for 1-4 min, as no stagnation of current density with low aluminum content (3 mass% Al, Figure 5(a)) was seen at *ca*. 2 mA·cm^{-2}, as is seen in pure magnesium. This

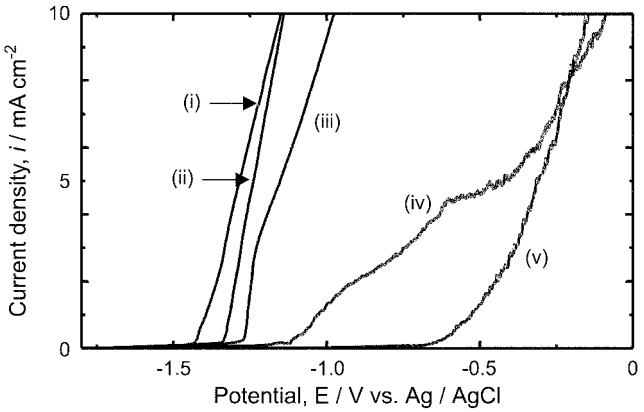

(i) Non-anodizing, (ii) 3 min, (iii) 5 min, (iv) 10 min, (v) 30 min

Figure 8. Anti-corrosion property with anodizing time for 15 mass% Al in 0.017 mol·dm^{-3} NaCl and 0.1 mol·dm^{-3} Na_2SO_4 solution at 298 K. Anodizing was carried out at conditions for 10 min at 3 V in 1 mol·dm^{-3} NaOH solution at 298 K.

was ascertained in SEM studies of the surface morphology (Figure 7(b)(i)). It seemed that a film formed on the α phase at a current density of approximately 10^2 mA·cm^{-2}, because all the specimens were similar, as seen by SEM (Figure 7(b)(ii, iii)). As compact films did not form on specimens anodized for 10 min, it appears that the current density increases in the anodic film formed on the α phase, beginning at around –1.2 V, because the anodic film formed in the α phase is a non-compacted film. Subsequently, the current density abruptly increased at a potential of –0.4 V (Figure 8). When anodized for 30 min, the anodic film on the α phase was more compact than that at 10 min. Therefore, with anodization for 30 min, the anodic polarization curve was the same shape as that for specimens anodized at other potentials. In addition, when anodized for more than 30 min, the polarization curves were similar to that for 30 min.

However, we were not convinced that the α and β phases are present in Figure 7. Therefore, EDX analysis was used to verify the presence of the α and β phases without (a) and with (b) anodization for 10 min at 3 V for 15 mass% Al in 1 mol·dm^{-3} NaOH, as shown in Figure 9. Without anodizing (a), the EDX analysis confirmed the phases in regions (1) and (2). The Al content in region (1) far exceeds that in region (2). This indicated that region (1) is the β phase and region (2) is the α phase. With anodizing (b), the Al content in regions (1) to (3) was in the order: region (2) » region (1) > region (3). Over time, the active dissolution reaction during anodizing occurred preferentially at the β phase until about 4 min. Then, the current density gradually increased until 7 min. The dissolution reaction progressed on α phase, which had a lower Al content.

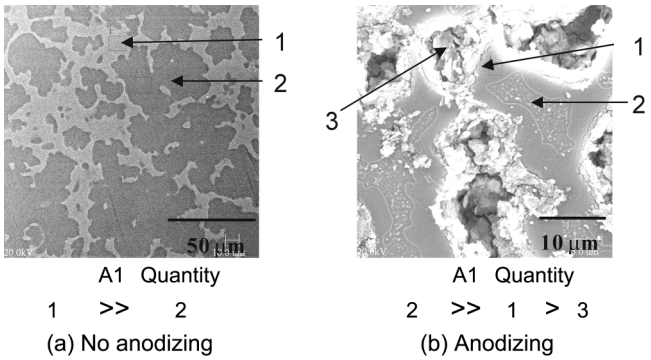

Figure 9. Surface morphologies in without (a) and with (b) anodized for 10 min at 3 V for 15 mass% Al in 1 mol·dm^{-3} NaOH solution at 298 K.

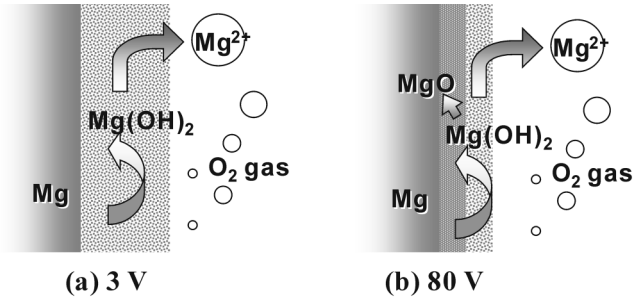

Figure 10. Schematic diagram on formation mechanism of anodic film.

These results suggest that the mechanism of anodic oxide film formation on a specimen of Mg-Al alloy anodized in 1.0 mol·dm^{-3} NaOH solution is as follows. Metal substrate/film and film/electrolyte interfaces occur during generation of the film (Figure 10). The interface at a low potential, like 3 V, is a metal substrate/film interface. The dissolution reaction of magnesium ($Mg \rightarrow Mg^{2+} + 2e^-$) occurs. The Mg quickly combines with OH^- in the NaOH solution ($Mg^{2+} + 2OH^- \rightarrow Mg(OH)_2$).

A MgO film formed at a high potential of 80 V, although extremely small $Mg(OH)_2$ peaks were also observed in the XRD analyses of specimens anodized at various constant potentials. The temperature at the specimen surface increased at high potentials, such as 80 V.[20] The reaction in formula (1) seen with increasing temperature is thought to be the partial reaction of $Mg(OH)_2$.

$$Mg(OH)_2 \rightarrow MgO + H_2O \quad (1)$$

Anodizing is accompanied by intensive sparking and oxygen evolution.[8,21,22] Therefore, formula (2) occurred at the film/electrolyte interface.

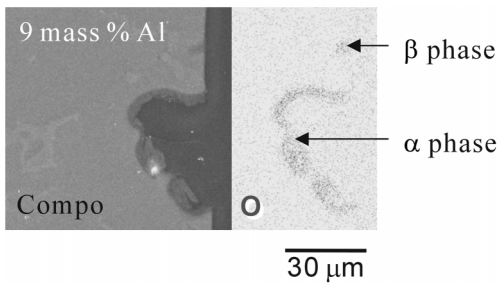

Figure 11. SEM photography and EDX analysis of cross section of Mg-9 mass%Al alloy anodized for 10 min at 3 V in 1 mol·dm^{-3} NaOH solution at 298 K.

$$Mg(OH)_2 \rightarrow Mg^{2+} + 1/2O_2\uparrow + H_2O + 2e^- \quad (2)$$

Figure 11 shows an EDX map of a cross-section of a specimen of Mg-9 mass% Al anodized for 10 min at 3 V in 1.0 mol·dm^{-3} NaOH at 298 K. The film that formed on the α phase was about 10 μm thick, *i.e.*, the oxygen region. This suggests that $Mg(OH)_2$ was generated in this region.

Conclusion

The anti-corrosion properties of anodized specimens were excellent, as compared with those of non-anodized specimens. When Mg-Al alloys were anodized, a $Mg(OH)_2$ film was primarily seen at an applied potential of 3 V, while a MgO film appeared at an applied potential of 80 V. The intensity ratio of the β phase increased with aluminum content in the Mg-Al alloys. Over time, the active dissolution reaction during anodizing occurred preferentially on the β phase until about 4 min. Then, the current density increased gradually with time until 7 min. After anodizing for 10 min, the current density increased when the aluminum content was 15 mass%, since the anodic film that forms on the α phase is a non-compact film. The anodic film on the α phase at 30 min was compact compared with that at 10 min.

Acknowledgements. The authors would like to acknowledge support for this research from the Japan Society for the Promotion of Science.

References

1. Suzuki, K. *Alutopia* **2000**, *5*, 40.
2. The European Parliament and Council; Draft proposal for a direct on the restriction of the use of certain hazardous substances in electrical and electronic equipment, June 2000.
3. Kunieda, N. 107th Meeting of the Surface Finishing Society of Japan, 2003; p 296.
4. Kim, S. J.; Okido, M. Sealing improved film properties after anodizing of Mg-Al alloys, *Bull. Korea Chem. Soc*. submitted.
5. Kim, S. J.; Okido, M.; Ichino, R.; Mizutani, Y.; Tanikawa, S.; Hasegawa, H. *Materials Transactions* **2003**, *44*, 1036.
6. Kim, S. J.; Zhou, T.; Ichino, R.; Okido, M.; Tanikawa, S. *Metals and Materials International* **2003**, *9*, 207.
7. Kim, S. J.; Hara, R.; Ichino, R.; Okido, M.; Wada, N. *Materials Transactions* **2003**, *44*, 782.
8. Emley, E. F. *Principle of Magnesium Technology*; Pergamon Press: London, 1966; p 122.
9. Huber, K. *J. Electrochem. Soc.* **1953**, *100*, 376.
10. Evangelides, H. A. *Metal Finishing* **1951**, *7*, 56.
11. Ono, S.; Asami, K.; Osaka, T.; Masuko, N. *J. Electrochem. Soc*. **1996**, *143*, L 62.
12. Khaselev, O.; Yahalon, J. *J. Electrochem. Soc*. **1998**, *145*, 190.
13. Khaselev, O.; Yahalon, J. *Corrosion Sci*. **1998**, *40*, 1149.
14. Oh, H. J.; Chi, C. S. *Bull. Korean Chem. Soc.* **2000**, *21*, 193.
15. Ono, S.; Kijima, H.; Masuko, N. *J. Japan Institute of Light Metals* **2002**, *52*, 115.
16. Ono, S.; Kijima, H.; Masuko, N. *J. of the Surface Finishing Society of Japan* **2000**, *51*, 1168.
17. Mizutani, Y.; Kim, S. J.; Ichino, R.; Okido, M. *J. Surf. & Coating Tech*. **2003**, *169-170*, 143.
18. Lunder, O.; Lein, J. E.; Aune, T. K.; Nisancioglu, K. *Corrosion* **1989**, *45*, 741.
19. Makar, G. L.; Kruger, J. *J. Electrochem. Soc*. **1990**, *137*, 414.
20. Zhang, Y.; Yan, C.; Wang, F.; Lou, H.; Cao, C. J. *Surf. & Coating Tech*. **2002**, *161*, 36.
21. Khaselev, O.; Weiss, D.; Yahalon, J. *J Electrochem. Soc*. **1999**, *146*, 1757.
22. Khaselev, O.; Weiss, D.; Yahalon, J. *Corrosion Sci*. **2001**, *43*, 1295.